Fabrication of fibrinogen/P(LLA-CL) hybrid nanofibrous scaffold for potential soft tissue engineering applications

Chuanglong He,[1,2,3] Xiaohong Xu,[2] Fan Zhang,[2] Lijun Cao,[2] Wei Feng,[2] Hongsheng Wang,[2] Xiumei Mo[1,2,3,4]

[1]State Key Laboratory for Modification of Chemical Fibers and Polymer Materials, Donghua University, Shanghai 201620, People's Republic of China
[2]College of Chemistry, Chemical Engineering and Biotechnology, Donghua University, Shanghai 201620, People's Republic of China
[3]Key Laboratory of Textile Science and Technology, Ministry of Education, Donghua University, Shanghai 201620, People's Republic of China
[4]State Key Laboratory of Bioreactor Engineering, East China University of Science and Technology, Shanghai, People's Republic of China

Received 1 September 2010; revised 9 January 2011; accepted 25 January 2011
Published online 4 April 2011 in Wiley Online Library (wileyonlinelibrary.com). DOI: 10.1002/jbm.a.33067

Abstract: Coelectrospinning of native proteins and elastic synthetic polymers is an attractive technique to fabricate hybrid fibrous scaffolds that combine the bioactivity and mechanical features of each material component. In this study, hybrid fibrous scaffolds composed of synthetic P(LLA-CL) elastomeric and naturally derived fibrinogen protein were fabricated and characterized for their bioactive and physiochemical properties. Fiber diameters of hybrid scaffolds increased with increasing P(LLA-CL) content, and the shape of fibers changed from cylindrical shape on pure polymer scaffolds to flat structure on hybrid scaffolds. Characterizations of ATR-FTIR, XRD, and thermal properties indicated that the hybrid scaffolds contain two different phases, one composed of pure fibrinogen and the other corresponding to a mixture of fibrinogen and P(LLA-CL), and no obvious chemical reaction takes place between two components. The hybrid fibrous scaffolds showed tailorable degradation rates than pure P(LLA-CL) and higher mechanical properties than pure fibrinogen, and both tensile strength and breaking strain increased with increasing P(LLA-CL) content. *In Vitro* studies revealed that L929 cells on hybrid scaffolds achieved relatively higher level of cell attachment after 12 h of culture and significant increased cell proliferation rate after 7 days of culture, when compared with pure fibrinogen and P(LLA-CL) scaffolds, and the cells exhibited a spreading polygonal shape on the hybrid fibrous surfaces compared to a round shape on surfaces of pure polymer scaffolds. Therefore, the fibrinogen/P(LLA-CL) hybrid fibrous scaffolds possess the combined benefits of each individual component, which make it capable as scaffolds for soft tissue reconstruction. J Biomed Mater Res Part A: 97A: 339–347, 2011.

Key Words: electrospinning, fibrinogen, P(LLA-CL), nanofibrous scaffold, soft tissue engineering

INTRODUCTION

In the engineering of soft tissues, scaffolds with high elasticity and strength coupled with favorable structural, biochemical, and biological properties are desirable.[1,2] This is particularly important when engineering mechanically active soft tissues like blood vessels, cardiac muscle and heart valves, as such scaffolds would provide effective mechanical stimuli between the cells and the scaffold and thus favor the development of functional soft tissues.[3,4]

Due to the stiffness and lack of elasticity, most of the commonly used synthetic polyesters such as poly(glycolic acid) (PGA), poly(lactic acid) (PLA), and their copolymers are not ideally suited for engineering soft tissues. Poly (epsilon-caprolactone) (PCL) is an exception and widely used for tissue engineering and drug delivery applications owing to its biocompatibility, biodegradability, and flexibility.[5–7] However, its low degradation rate and hydrophobicity limited the efficacy of PCL as a scaffold for soft tissue engineering. The copolymerization of PCL with PLA and PGA can produce novel material which will capable to provide better control over the degradation and mechanical properties while retaining good biocompatibility.[8,9] In recent years,

Correspondence to: C. He; e-mail: hcl@dhu.edu.cn
Contract grant sponsor: Natural Science Foundation of Shanghai; contract grant number: 07ZR14001
Contract grant sponsor: Shanghai-Unilever Research and Development Fund; contract grant number: 08520750100
Contract grant sponsor: Fundamental Research Funds for Central Universities, Ministry of Education of China; contract grant number: 200802551014
Contract grant sponsor: Open Foundation of State Key Laboratory for Modification of Chemical Fibers and Polymer Materials; contract grant number: LK0804
Contract grant sponsor: State Key Laboratory of Bioreactor Engineering, China; contract grant number: B07024

poly(L-lactic acid)-co-poly (epsilon-caprolactone) (P(LLA-CL)) has received considerable attention as a suitable scaffolding material in vascular,[9–11] neural[12] and tendon/ligament tissue engineering,[13] since it possess appropriate elasticity and flexibility, and tailorable degradation properties by altering lactic acid (LA) and caprolactone (CL) ratio. This has led to successfully engineering of mechanically active artificial vascular graft. For example, Inoguchi et al.[8] demonstrated the P(LLA-CL) tubular scaffolds could pulsate synchronously by responding to pulsatile flow which approached that of a native artery. Nonetheless, like other synthetic polymers, P(LLA-CL) lack cell recognition and adhesion sites which results in poor cell affinity.[14,15] To overcome this problem, several natural polymers including collagen,[16,17] gelatin,[18] chitosan,[19] and silk fibroin[20] have been introduced in the P(LLA-CL) scaffolds by either surface coating or physically blending, which could improve the biocompatibility of the P(LLA-CL) scaffolds without sacrificing their mechanical strength, thus integrating the advantages of two types of materials.

Fibrinogen is a 340-kDa plasma glycoprotein that plays a key role in blood clotting and wound healing.[21] In physiological conditions, when a body tissue or blood vessel wall is injured, fibrinogen can undergo a complex coagulation cascade to assembly into insoluble fibrin fibrous structures, these fibrous structures can be regarded as a unique nature's provisional matrix on which tissues rebuild and repair themselves, making them an attractive scaffold for tissue engineering.[22–25] Fibrinogen-based materials have been widely used in the tissue engineering of cartilage,[26] bone,[27] skin,[28] and blood vessel,[29] etc. as hydrogel type biomaterials, mainly due to their innate ability to induce cellular interaction and subsequent tissue remodeling. However, the major disadvantage of using fibrin gels is difficult to construct scaffolds with structural integrity and sufficient mechanical strength over time.[23,30] To this end, electrospun fibrinogen nanofibers have been recently developed as scaffolds for specific tissue engineering applications that have been shown to support cell proliferation and to promote cell interaction, but the rapid degradation of thus materials is still a challenge for engineering of mechanically active soft tissues.[30,31]

The rapid growth of electrospinning technique has opened a new era of processing a range of biomaterials into sub-microscale or nanoscale fibers which resemble that of the native tissues. The resultant matrices can be manipulated into a complex construct with desired chemical compositions and physical architectures by selecting suitable material components along with processing parameters.[32,33] More importantly, the scaffolds can be readily integrated with biological, chemical, and mechanical cues to provide favorable biomimetic milieu for optimized cell and tissue responses. Our previous studies[19,20] have shown that P(LLA-CL) could be readily coelectrospun with several natural polymers to generate hybrid scaffolds, which have improved biocompatibility and mechanical properties than single-component scaffolds due to synergistic interaction between two materials.

To overcome limitations of each single-component scaffold, we developed novel P(LLA-CL)/fibrinogen hybrid fibrous scaffolds that combine both the merits of the desirable elasticity and flexibility of P(LLA-CL) and the good biocompatibility of fibrinogen. These fibrous scaffolds were fabricated by coelectrospinning of two materials in different weight ratios. Their morphologies were observed by scanning electron microscope (SEM). Their composition, physiochemical properties and mechanical properties were characterized by attenuated total reflectance-Fourier transform infrared spectra (ATR-FTIR), X-ray diffraction (XRD), thermal gravimetric (TG) analysis, water contact angle, *in vitro* degradation, and tensile strength tests, respectively. Furthermore, their *in vitro* biocompatibility including cell viability, adhesion, and proliferation were evaluated and compared by using mouse fibroblasts (L929 cells).

MATERIALS AND METHODS

Materials

The block copolymer of P(LLA-CL) (M_w = 1.3–1.4 × 10^5, Japan) comprised of 75 mol % L-lactide and 25 mol % epsilon-caprolactone monomers was used. Fibrinogen (Fibrin Sealant®, derived from porcine blood) was obtained from Guangzhou Bioseal BioTech (China). 1,1,1,3,3,3,-hexafluoro-2-propanol (HFIP) of analytical grade was purchased from Daikin Industries (Japan). Mouse fibroblasts (L929) were obtained from institute of biochemistry and cell biology (Chinese Academy of Sciences, China). All culture media and reagents were purchased from Gibco Life Technologies (USA).

Scaffold fabrication by electrospinning

Fibrinogen solution was prepared by dissolving fibrinogen powders into a mixture of HFIP and Dulbecco's modified eagle medium (DMEM) with a volume ratio of 9:1, and P(LLA-CL) solutions were also obtained by dissolving P(LLA-CL) pellets in HFIP. Both solutions were stirred overnight until the solution became homogeneous. Then, a series of fibrinogen/P(LLA-CL) blend solutions with different weight ratios (80/20, 60/40, 40/60, and 20/80, respectively) were prepared by mixing each solution in appropriate ratios. The total polymer concentration in blend solutions was kept at 12 wt %, whereas pure fibrinogen and P(LLA-CL) scaffolds were electrospun using 18 and 8 wt %, respectively. These concentrations were selected based on our pilot experiments, and represented the optimum concentration for electrospinning.

All electrospinning experiments were performed at room temperature. The prepared solution was respectively loaded into a 5-mL plastic syringe with a stainless steel needle (inner diameter, 0.21 mm) attached. The needle was connected to a high-voltage supply (BGG6-358, BMEI, China). The solution was fed at 0.8 mL/h using a syringe pump (789100C, Cole-Parmer Instruments, USA). A plate of aluminum foil was grounded and placed 13 cm below the needle tip, and used to collect nanofibers. The voltage for electrospinning was set at 20 kV. The thicknesses of all resulting nanofibrous mats were controlled at around 0.1 mm. These fibers were then dried in a *vacuum* for 48 h to remove the residual solvents.

Morphology

The morphologies of electrospun fibers were observed with scanning electron microscope (SEM, Hitachi S-2700, Japan) at an accelerating voltage of 10 kV. Prior to SEM observation, all of the samples cut from the electrospun scaffolds were sputter coated with gold for 60 s. The diameters of nanofibers were measured based on SEM images using image visualization software (ImageJ 1.34s, NIH Image, USA). The average fiber diameter and its distribution were determined from about 100 measurements on a typical SEM image.

ATR-FTIR

The nanofibrous scaffolds were characterized by attenuated total reflectance-Fourier transform spectroscopy (Avatar380, USA). The infrared spectra of the samples were measured over a wavelength range of 4,000–500 cm^{-1} with a resolution of 4 cm^{-1}.

Wide-angle X-ray diffraction

XRD data were collected using a diffractometer (Rigaku D/max 2550PC, Japan) with Cu Kα radiation (40 kV, 100 mA). The diffraction scans were recorded at $2\theta = 5$–50° with a scanning rate of 6°/min.

Thermal analysis

TGA were conducted on a Perkin-Elmer TGA7 thermal analyzer (USA), about 2–3 mg sample was used in an aluminum pan and heated at a rate of 10°C/min from ambient temperature to 600°C in a nitrogen atmosphere. The nitrogen gas flow rate was 40 mL/min.

Contact angle measurements

Surface wettability of the electrospun scaffolds was characterized by the water contact angle measurement. The images of the droplet on the membrane were visualized through the image analyzer (OCA40, Dataphysics, Germany) and the angles between the water droplet and the surface were measured. The measurement used distilled water as the reference liquid and was automatically dropped onto the electrospun scaffolds. To confirm the uniform distribution of nanofibrous scaffolds, the contact angle was measured three times from different positions and an average value was calculated by statistical method.

In vitro degradation

For *in vitro* degradation study, the dried nanofibrous scaffolds were cut into 2×2 cm^2 samples and placed in 15-mL centrifuge tubes with 5 mL of sterile phosphate-buffered saline (PBS, pH 7.4) after accurately weighting, the tubes were subsequently placed inside an orbital incubator a 37°C, rotating at 60 rpm, for up to 21 days. At predetermined intervals, triplicate specimens for each sample condition were taken out of solutions and lyophilized to constant weight. The weight loss percentages were calculated from the dried weights obtained before and after degradation.

Tensile testing

For mechanical test, the samples were prepared according to our previous study.[7] A straight-line sample with a planar area of 50×10 mm^2 was cut from the nanofiber membrane, each end of which was glued in between two pieces of 10×10 mm^2 tapes, leaving a gauge length of 30 mm. The tensile testing was performed using a universal materials tester (H5 K-S, Hounsfield, UK) with a 50*N* load cell at ambient temperature 25°C and humidity 65%. A cross-head speed of 10 mm/min was used for all the specimens. For each group, at least five specimens were tested to calculate the mean value and standard deviation.

Cell culture and seeding

The thawed L929 mouse fibroblasts were cultured in a 5% CO_2, humid atmosphere at 37°C in DMEM medium containing 10% fetal serum, 100 units/mL penicillin and 100 units/mL streptomycin, the culture medium was changed every other day.

For *In vitro* biocompatibility assessment, the coverslips with 14 mm in diameter were placed onto the aluminum foil to collect the nanofibrous scaffolds, the thickness of scaffolds was ~0.1 mm. The scaffolds were then fixed in the 24-well plate with stainless steel rings and sterilized with 75% alcohol solution for 4 h, washed three times with phosphate-buffered saline solution (PBS) for 30 min each, and twice with cell culture medium for 1 h each.

Cell adhesion and proliferation assays

For cell adhesion study, L929 mouse fibroblasts (5×10^4/mL) were seeded onto nanofibrous scaffolds with coverslips as control. After 2, 4, 6, and 12 h of culture, each sample was rinsed with PBS to remove unattached cells. The cell-scaffold composites were evaluated by MTT assay at the absorbance of 570 nm by using an enzyme-labeled instrument (MK3, Thermo, USA). For proliferation study, 5×10^4 cells were seeded on the scaffolds with coverslips as control. The proliferation of the cells on each specimen was determined after varying culture period of 1, 3, and 5 days, respectively. The viability of the cells was quantified by MTT assay at the absorbance of 570 nm. Morphological appearance of the cells after 3 days of culture was observed by SEM (Hitachi S-2700, Japan). Cells cultured on scaffolds were washed with PBS and then fixed with 4% glutaraldehyde overnight at 4°C. The samples were dehydrated in 50, 75, and 100% alcohol solutions and dried under vacuum. Afterwards, the samples were sputter coated with gold and examined using a SEM at voltage of 15 kV.

Statistical analysis

All experiments were conducted at least three times and all values were reported as the mean and standard deviation. Statistical analysis was carried out by the one-way analysis of variance (one-way ANOVA) and Scheffe's *post hoc* test in SPSS (SPSS). The statistical difference between two sets of data was considered when $p < 0.05$.

RESULTS AND DISCUSSION

Fiber morphology

In general, the morphology and size of electrospun fibers are affected by various parameters including the applied voltage, feeding rate, collecting distance, and especially the properties of the polymer solutions and solvents.[7,34] To enhance electrospinability, the appropriate solvent system for simultaneously dissolving two different polymers is preferred during coelectrospinning of two polymers. HFIP is an ideal solvent for a variety of natural polymers, in which both fibrinogen and P(LLA-CL) can readily dissolve to form a homogenous solution. Additionally, it can be evaporated completely after jet solidification and thus leave fewer residues on the resultant fibers.[1] The processing parameters were optimized according to our previous studies on electrospinning of fibrinogen. Figure 1 shows the fibrous morphologies of the formed electrospun scaffolds, which were found to be porous mats with random aligned fibers. However, the shape and surface morphology of the fibers was changed with the blend ratio of two polymers. The fibers fabricated from single-component polymer have a cylindrical shape, whereas hybrid fibers show a flat structure with a larger diameter distribution. For example, in the case of fibrinogen/P(LLA-CL) (80/20) [Fig. 1(b)], fibers showed a flat structure and were attached to each other. Furthermore, the content of small diameter fibers increased with increasing content of P(LLA-CL). When the ratio of P(LLA-CL) was increased to 80, fibrinogen/P(LLA-CL) (20/80) [Fig. 1(e)] scaffolds showed that some small size fibers appeared and entangled with large fibers, and the fraction of small size fibers increased by increasing content of P(LLA-CL). Figure 2 shows the average fiber diameters and their distribution determined from the SEM images. Fiber diameters were 145 $\pm$ 48, 174 $\pm$ 64, 219 $\pm$ 86, 262 $\pm$ 65, 305 $\pm$ 78, and 644 $\pm$ 225 nm for fibrous mats containing P(LLA-CL) of 0, 20, 40, 60, 80, and 100%, respectively. Fiber diameter was found to increase with increasing content of P(LLA-CL) in hybrid scaffolds.

ATR-FTIR analysis

Figure 3 shows the ATR-FTIR spectra of fibrinogen [Fig. 3(a)], P(LLA-CL) [Fig. 3(f)], and fibrinogen/P(LLA-CL) at different blend ratios fibrous scaffolds [Fig. 3(b–e)]. From the spectra of fibrinogen/P(LLA-CL) hybrid scaffolds, the peaks at 1650 and 1540 cm^{-1} correspond to the amide I and amide II bands of fibrinogen, which are characteristic peaks of proteins with high α-helix content.[35] The peak at 1760 cm^{-1} is attributed to the C=O stretching vibration of P(LLA-CL), and its intensity increased with higher P(LLA-CL) content. The combined results confirmed that the hybrid scaffolds contained two different components and no obvious chemical reaction occurs between two components.

XRD analysis

Figure 4 shows XRD patterns of electrospun fibrinogen [Fig. 4(a)], P(LLA-CL) [Fig. 4(f)], and their blends [Fig. 4(b–e)]. Electrospun fibrinogen exhibited two main diffraction peaks at 11.6 and 21.1° and a small peaks at 24.1°, while electrospun P(LLA-CL) showed a sharp peak at 2θ of 16.4° and two relatively low intensity peak at 18.9 and 22.1°. For fibrinogen/P(LLA-CL) nanofibers [Fig. 4(b–e)], only a peak at 11.6° was clearly observed, but a wide and low intensity peak at 16.4° became remarkable for blends with higher P(LLA-CL) content. These results indicated that the hybrid nanofibrous scaffolds were in lower crystallization, this is probably attributed to rapid solidification of the stretched chains at high elongational rates during the electrospinning

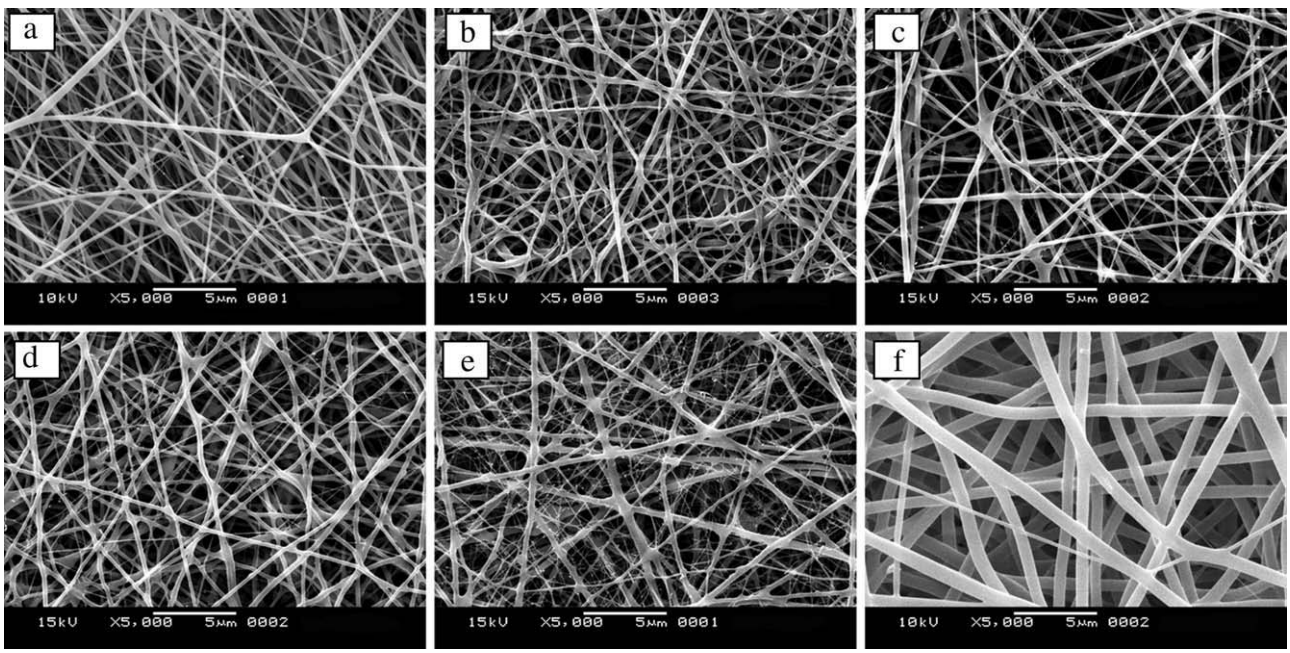

FIGURE 1. SEM images of fibrous scaffolds with different blend ratios of fibrinogen to P(LLA-CL). (a) 100:0, (b) 80:20, (c) 60:40, (d) 40:60, (e) 20:80, and (f) 0:100. The scale bar shown in all images is 5 μm.

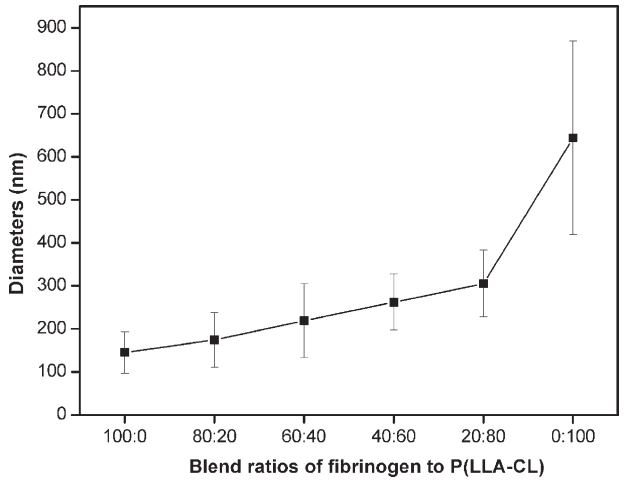

FIGURE 2. Diameter distribution of fibrous scaffolds with different blend ratios of fibrinogen to P(LLA-CL). (a) 100:0, (b) 80:20, (c) 60:40, (d) 40:60, (e) 20:80, and (f) 0:100.

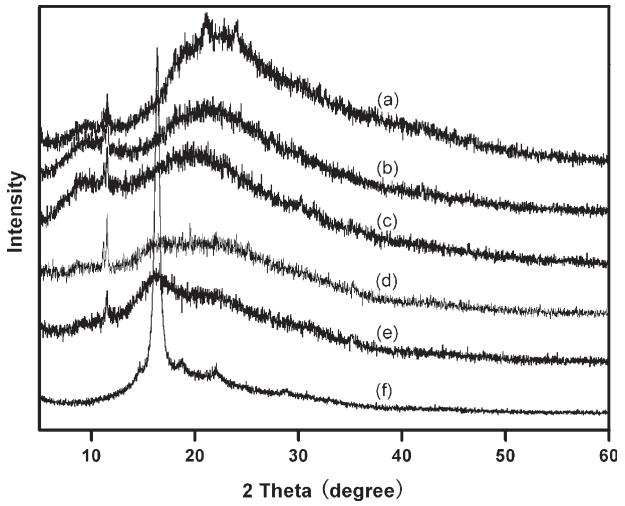

FIGURE 4. XRD patterns of fibrous scaffolds with different blend ratios of fibrinogen to P(LLA-CL). (a) 100:0, (b) 80:20, (c) 60:40, (d) 40:60, (e) 20:80, and (f) 0:100.

process, and the stretched chains have insufficient time to form a crystalline structure before they are solidified.[36]

Thermal properties

The thermal stability of the fibrous mats was studied by TG and derivative thermal gravimetric (DTG) analysis. Figure 5 shows the TG curve for the thermal degradation of electrospun fibrinogen [Fig. 5(a)], P(LLA-CL) [Fig. 5(f)], and their blends [Fig. 5(b–e)]. Apparently, blend fibers showed an intermediate decomposition pattern compared to their pure components. Figure 6 shows the thermograms made on the basis of the first derivative of the TG plots. DTG curve of electrospun fibrinogen [Fig. 6(a)] presents at least three decomposition stages with maximum rates at around 133, 228, and 302°C, while only one degradation peak for the P(LLA-CL) nanofibers appears at 346°C [Fig. 6(f)]. For fibrinogen/P(LLA-CL) (80/20) nanofibers [Fig. 6(b)], only one peak for fibrinogen was observed at 228°C. However, a new main decomposition peak at around 280°C was observed and became more apparent for other blends with higher P(LLA-CL) content, as shown in Figure 6(c–e). These results suggest that two phases, one composed of pure fibrinogen and the other corresponding to a mixture of fibrinogen and P(LLA-CL), coexist in the fibrinogen/P(LLA-CL) nanofibers. The formation of two phases in hybrid scaffolds may be caused by partially phase separation of two different components during the rapid solvent evaporation process, which results in some fibrinogen phases being migrated to the outside of the hybrid fibers, and thus forming some small size fibers. These results agree with the SEM morphology observation as shown in Figure 1.

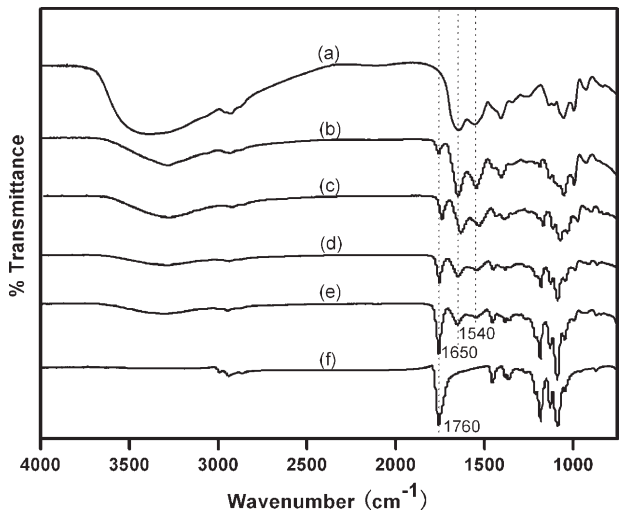

FIGURE 3. ATR-FTIR spectra of fibrous scaffolds with different blend ratios of fibrinogen to P(LLA-CL). (a) 100:0, (b) 80:20, (c) 60:40, (d) 40:60, (e) 20:80, and (f) 0:100.

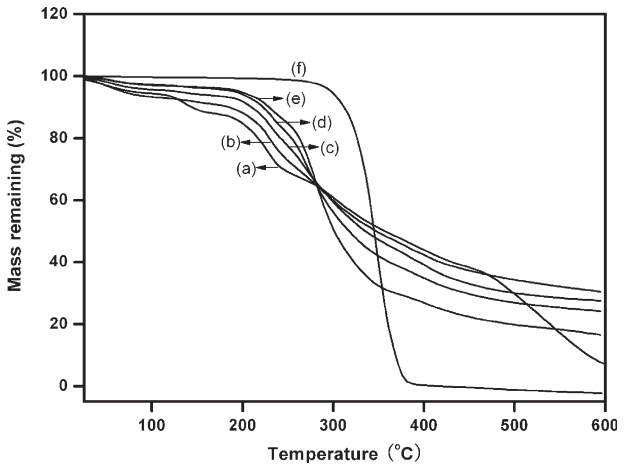

FIGURE 5. Thermal gravimetric analysis of fibrous scaffolds with different blend ratios of fibrinogen to P(LLA-CL). (a) 100:0, (b) 80:20, (c) 60:40, (d) 40:60, (e) 20:80, and (f) 0:100.

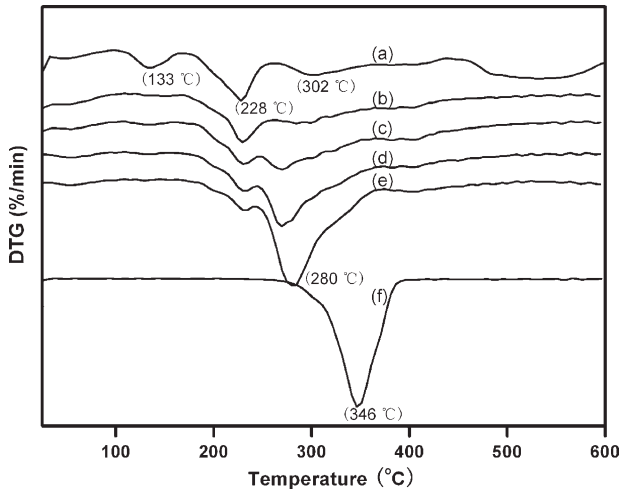

FIGURE 6. Derivative thermal gravimetric analysis of fibrous scaffolds with different blend ratios of fibrinogen to P(LLA-CL). (a) 100:0, (b) 80:20, (c) 60:40, (d) 40:60, (e) 20:80, and (f) 0:100.

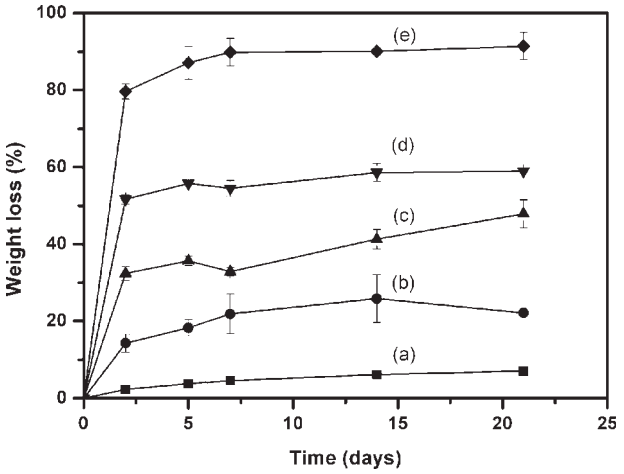

FIGURE 8. Weight loss of fibrous scaffolds with time after incubating in phosphate buffered saline (pH 7.4) at 37°C for up to 21 days, the blend ratios of P(LLA-CL) to fibrinogen in scaffolds were (a) 100:0, (b) 80:20, (c) 60:40, (d) 40:60, and (e) 20:80. Data are means ± SD ($n = 3$).

Water contact angle analysis

The surface wettability plays an important role in cell adhesion, spreading, and proliferation on the biomaterials surfaces.[17,37] To determine the influence of different blending ratios on the surface wettability of electrospun fibrinogen/P(LLA-CL) scaffolds, the contact angle measurement was done and shown in Figure 7. The pure electrospun fibrinogen scaffolds showed a contact angle of about 64°, indicating that the surface was hydrophilic. In contrast, the electrospun P(LLA-CL) scaffolds exhibited more hydrophobic properties, which has a contact angle of ~129°. As the P(LLA-CL) content increased from 20 to 80%, the contact angle of hybrid scaffolds increased from 75 to 100°. Therefore, the surface wettability of hybrid scaffolds can be tailored by changing the ratio of two components in the blend.

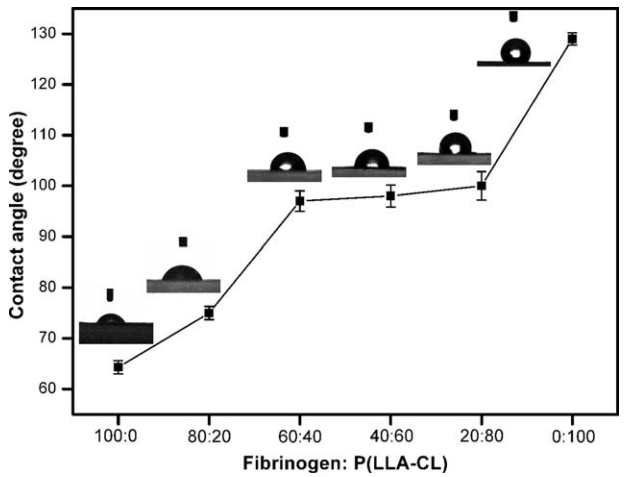

FIGURE 7. Water contact angles of fibrous scaffolds with different blend ratios of fibrinogen to P(LLA-CL) (Inset in this figure shows the variation of contact angle on different scaffolds). Data are means ± SD ($n = 3$).

In vitro degradation

The *in-vitro* degradation of electrospun scaffolds was determined by the weight loss of the fibrous samples during the course of degradation. Figure 8 shows the weight loss of various scaffolds as a function of incubation time in PBS at 37°C, and the data for pure fibrinogen scaffold was not included since it dissolved completely in PBS within the first 2 days of incubation. For all fibrinogen-contained scaffolds, the degradation of scaffolds involves a two-stage process consisting of a sharp initial weight loss at the first week of incubation followed by a smooth degradation, the mass loss of the scaffolds in the early stage may result from the dissolution of fibrinogen into the medium. In addition, the degradation rate of hybrid scaffolds increased significantly with the increase of fibrinogen content in scaffolds. For example, the scaffold containing 80% fibrinogen showed a percentage weight loss of 91.4% after degradation for 21 days as compared to 22.2% weight loss of the scaffolds containing 20% fibrinogen at the same time point. Pure P(LLA-CL) scaffolds showed a slow degradation rate when compared to the hybrid scaffolds, only 7.1% of weight loss was detected after 21 days of incubation. These results indicated that the hydrophilicity and degradation property of the prepared fibrinogen/P(LLA-CL) scaffolds can be tuned by changing the content of fibrinogen in scaffolds.

Mechanical properties

Mechanical properties of scaffolds are critical for their successful application in engineering soft tissue. For example, a major cause of graft failure in synthetic vascular grafts is intimal hyperplasia, which is often caused by the compliance mismatch between the graft and the host blood vessel.[38] Therefore, the appropriate mechanical compatibility between synthetic scaffolds and host tissues is a requirement for well functioning soft tissue substitutes.

Figure 9 shows the typical tensile stress–strain curve of electrospun fibrinogen, P(LLA-CL), and hybrid scaffolds. The

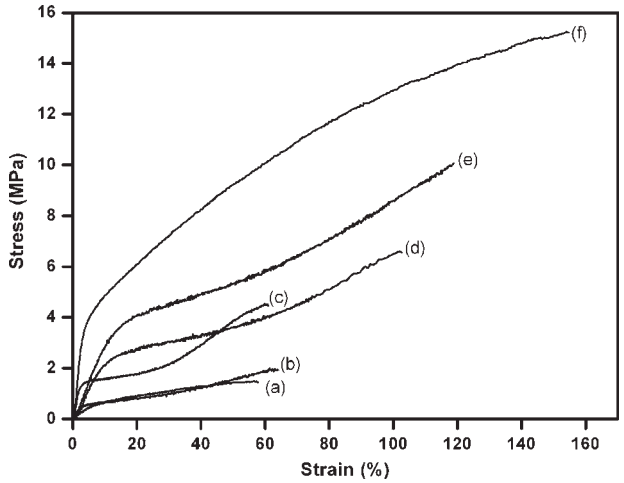

FIGURE 9. Typical tensile stress–strain curve of fibrous scaffolds with different blend ratios of fibrinogen to P(LLA-CL). (a) 100:0, (b) 80:20, (c) 60:40, (d) 40:60, (e) 20:80, and (f) 0:100.

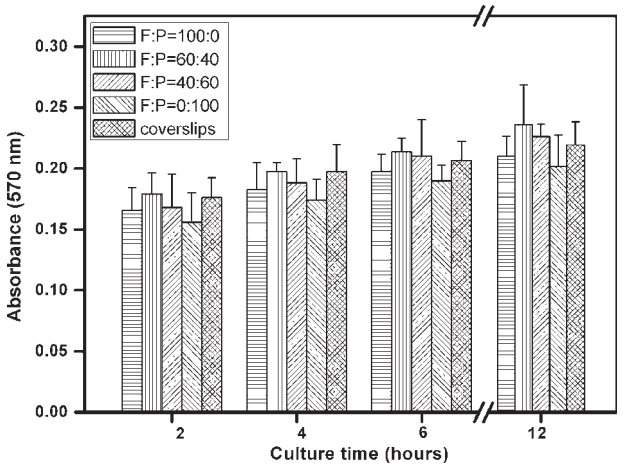

FIGURE 10. Attachment of L929 cells on the surfaces of fibrous scaffolds and coverslips (as control) after 2, 4, 6, and 12 h of seeding. (The letter F and P in the figure represent fibrinogen and P(LLA-CL), respectively).

tensile strength and ultimate strain are summarized in Table I. The average tensile strength of P(LLA-CL) scaffolds was 15.1 MPa with an ultimate strain of 160.4% when compared with 1.6 MPa and 57.7% for fibrinogen, indicating that both materials possess distinct mechanical properties. Fibrinogen is readily degraded by plasmin and other metalloproteinases found in serum, the mechanical strength of fibrinogen scaffold can be improved by chemical cross-linking or media supplementation with aprotinin.[24,30,31] However, these treatments may result in some harmful effects such as increased cytotoxicity since some commonly used cross-linkers are toxic even in relatively low concentration.[31] In the present study, all the hybrid scaffolds showed higher tensile strength and ultimate strain than fibrinogen scaffolds, both tensile strength and ultimate strain increased with increasing the blend ratio of P(LLA-CL) to fibrinogen. Thus, it is possible to create hybrid scaffolds with desirable mechanical property and biocompatibility for engineering of various soft tissues, by selecting the optimum blend ratios of two components. The hybrid scaffolds with P(LLA-CL) content of 40 and 60% were selected for cell culture studies as they exhibited better comprehensive properties including hydrophilicity, degradation rate, and mechanical strength than other ones.

Attachment of L929 cells on nanofibers

Figure 10 shows the attachment of L929 cells on the surfaces of the fibrous scaffolds and coverslips (as control) after 2, 4, 6, and 12 h of seeding, respectively. L929 cells began to adhere to the fibrous scaffolds or coverslips after 2 h of culture, and more cells attached with increasing the incubation time from 2 to 12 h. At any given time points, pure P(LLA-CL) scaffolds showed the weak adhesion for cells due to its poor hydrophilicity, and the hybrid scaffolds containing 60% fibrinogen achieved a better adhesion than those of other fibrous scaffolds and coverslips, but there were no significant difference within 12 h among all tested materials.

TABLE I. Tensile Properties of Fibrinogen/P(LLA-CL) Nanofibers with Various Blend Ratios

Fibrinogen/P (LLA-CL) (w/w)	Tensile Stress (MPa)	Breaking Strain (%)
100:0	1.6 ± 0.1	57.7 ± 0.6
80:20	1.9 ± 0.4	60.5 ± 9.1
60:40	4.5 ± 0.5	65.6 ± 5.8
40:60	6.6 ± 0.9	103.2 ± 10.3
20:80	10.1 ± 0.4	118.8 ± 12.3
0:100	15.1 ± 2.3	160.4 ± 18.9

Viability and morphology of fibroblasts

Figure 11 shows the proliferation of L929 cells on the surfaces of the fibrous scaffolds and coverslips (as control) on days 1, 3, 5, and 7 after cell culturing. It can be seen that the cells proliferated on the fibrous scaffolds were higher

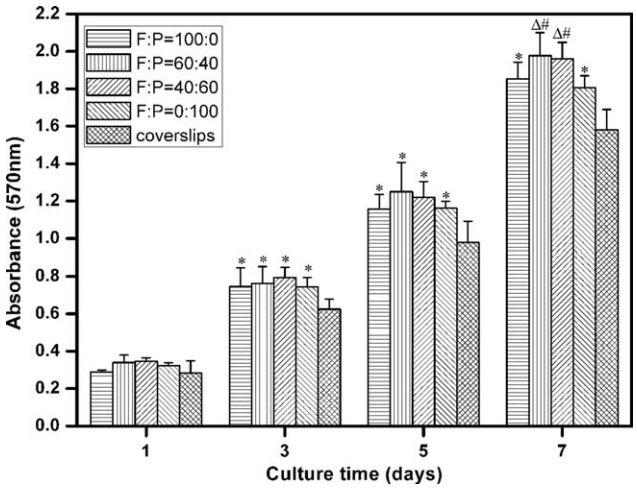

FIGURE 11. Proliferation of L929 cells on the surfaces of the fibrous scaffolds and coverslips (as control) on days 1, 3, 5, and 7 after cell culturing. ($^{*}p < 0.05$ and $^{\#}p < 0.10$ versus coverslips, $^{\Delta}p < 0.05$ versus pure fibrinogen and P(LLA-CL) scaffold. The letter F and P in the figure represent fibrinogen and P(LLA-CL), respectively).

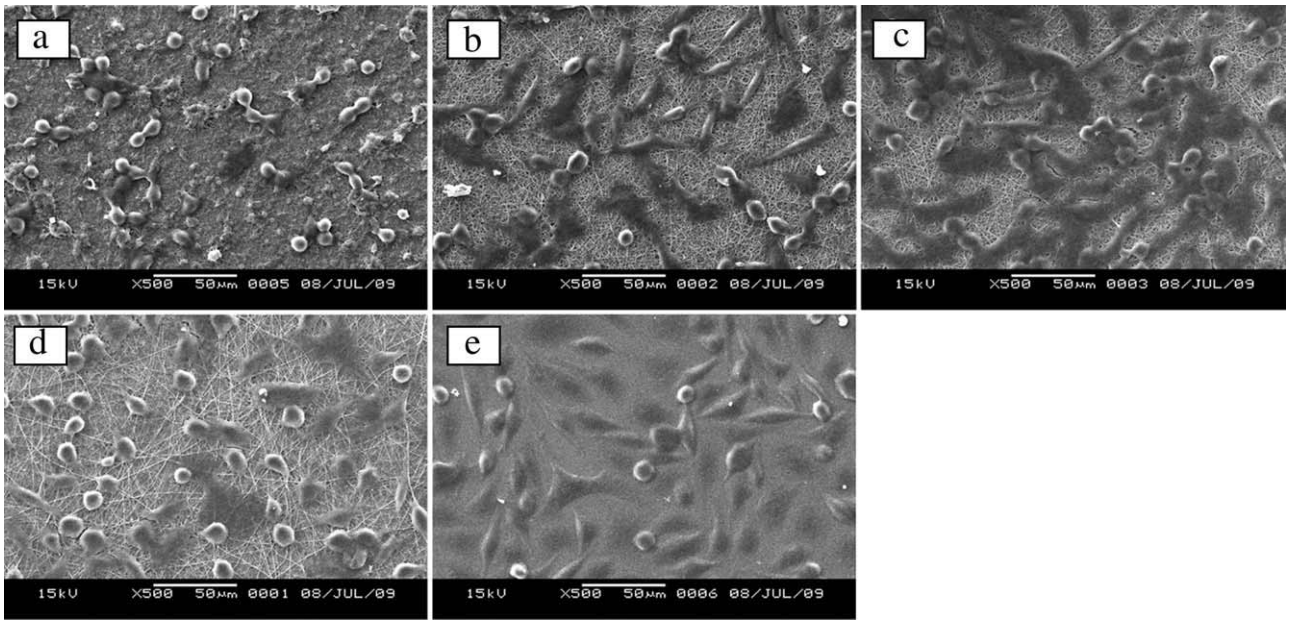

FIGURE 12. SEM images of L929 cells grown on fibrous scaffolds after culture for 3 days. (a) fibrinogen, (b) fibrinogen/P(LLA-CL) (60:40), (c) fibrinogen/P(LLA-CL) (40:60), (d) P(LLA-CL), and (e) coverslips. The scale bar shown in all images is 50 μm.

than that on the coverslips, but no significant difference among all tested materials was recognized at day 1. On days 3 and 5, cell proliferation on all fibrous scaffolds significant increased than that on the coverslips. On day 7, Cell proliferation on fibrinogen/P(LLA-CL) hybrid scaffolds (60:40 and 40:60) exhibited greater significant increase comparing to coverslips at the $p < 0.01$, while the significant difference in the cell proliferation activity between two pure fibrous scaffolds and coverslips is only at $p < 0.05$. In addition, cell proliferation on fibrinogen/P(LLA-CL) hybrid scaffolds (60:40 and 40:60) appeared significant difference when compared with pure fibrinogen and P(LLA-CL) scaffolds ($p < 0.05$). The results revealed that the hybrid scaffolds present better affinity to L929 cells than the pure fibrinogen and P(LLA-CL) scaffolds. This can be explained that the hybrid scaffolds provide the better hydrophilicity and biocompatibility compared to pure P(LLA-CL) scaffolds, and better structural integrity and mechanical properties than pure fibrinogen scaffolds, which favor the attachment and proliferation of L929 cells during the cell culturing.

Figure 12 shows SEM images of cultured cells on the fibrous scaffolds after a 3-day culture. It is noted that the fibrous structure of pure fibrinogen scaffold was almost disappeared and the scaffold porosity decreased after culture for 3 days, as shown in Figure 12(a). Similar results were reported by Sell et al.[39] who also concluded that electrospun fibrinogen scaffolds densify and contract when placed in an aqueous solution. Compared with L929 cells on pure fibrinogen and P(LLA-CL) scaffolds, on which more cells adopted a rounded and poor spread shape, L929 cells on two hybrid scaffolds (60:40 and 40:60) showed a spreading polygonal shape that is typical of normal cell morphology on coverslips [Fig. 12(e)]. The poor cell spread on pure fibrinogen scaffolds is mainly due to the strong time-dependent shrinkage of scaffolds in cell culture medium, making it fail to provide stable anchor sites for cell adhesion and spread. Whereas, lack of cell recognition sites on P(LLA-CL) nanofibers leads to the similar cell phonetype. Therefore, fibrinogen-blended P(LLA-CL) nanofibers showed great potential as scaffolds for soft tissue engineering because they can promote good fibroblast viability, attachment, and phenotypic maintenance of cells.

CONCLUSION

In this study, fibrinogen/P(LLA-CL) hybrid scaffolds with various blend ratios were prepared by electrospinning technique. The average diameters of blend nanofibers increased from 174 to 305 nm as the content of P(LLA-CL) increased from 20 to 80%. The results of ATR-FTIR, XRD, and thermal properties indicated that the fibrinogen/P(LLA-CL) hybrid scaffolds contain two different phases, one composed of pure fibrinogen and the other corresponding to a mixture of fibrinogen and P(LLA-CL), and no obvious chemical reaction occurs between two components. The hybrid nanofibrous scaffolds provided better hydrophilic than pure P(LLA-CL) and higher mechanical properties to pure fibrinogen. In addition, the hybrid scaffolds also provided better microenvironments for cell attachment, spreading, and proliferation. Therefore, the fibrinogen/P(LLA-CL) hybrid nanofibrous scaffolds, especially the ones containing P(LLA-CL) content of 40 and 60%, have the combined advantageous over each of individual component, which made them promising candidates as scaffolds for soft tissue reconstruction.

REFERENCES

1. Heydarkhan-Hagvall S, Schenke-Layland K, Dhanasopon AP, Rofail F, Smith H, Wu BM, Shemin R, Beygui RE, MacLellan WR. Three-dimensional electrospun ECM-based hybrid scaffolds for

cardiovascular tissue engineering. Biomaterials 2008;29: 2907–2914.
2. Guan JJ, Fujimoto KL, Sacks MS, Wagner WR. Preparation and characterization of highly porous, biodegradable polyurethane scaffolds for soft tissue applications. Biomaterials 2005;26: 3961–3971.
3. Guan J, Fujimoto KL, Wagner WR. Elastase-sensitive elastomeric scaffolds with variable anisotropy for soft tissue engineering. Pharm Res 2008;25:2400–2412.
4. Courtney T, Sacks MS, Stankus J, Guan J, Wagner WR. Design and analysis of tissue engineering scaffolds that mimic soft tissue mechanical anisotropy. Biomaterials 2006;27:3631–3638.
5. Kweon H, Yoo MK, Park IK, Kim TH, Lee HC, Lee HS, Oh JS, Akaike T, Cho CS. A novel degradable polycaprolactone networks for tissue engineering. Biomaterials 2003;24:801–808.
6. Hutmacher DW, Schantz T, Zein I, Ng KW, Teoh SH, Tan KC. Mechanical properties and cell cultural response of polycaprolactone scaffolds designed and fabricated via fused deposition modeling. J Biomed Mater Res 2001;55:203–216.
7. Huang ZM, He CL, Yang AZ, Zhang YZ, Hang XJ, Yin JL, Wu QS. Encapsulating drugs in biodegradable ultrafine fibers through coaxial electrospinning. J Biomed Mater Res 2006;77A:169–179.
8. Inoguchi H, Kwon IK, Inoue E, Takamizawa K, Maehara Y, Matsuda T. Mechanical responses of a compliant electrospun poly (L-lactide-*co*-(epsilon)-caprolactone) small-diameter vascular graft. Biomaterials 2006;27:1470–1478.
9. Mo XM, Xu CY, Kotaki M, Ramakrishna S. Electrospun P(LLA-CL) nanofiber: A biomimetic extracellular matrix for smooth muscle cell and endothelial cell proliferation. Biomaterials 2004;25: 1883–1890.
10. Nottelet B, Pektok E, Mandracchia D, Tille JC, Walpoth B, Gurny R, Moller M. Factorial design optimization and in vivo feasibility of poly(epsilon-caprolactone)-micro- and narofiber-based small diameter vascular grafts. J Biomed Mater Res 2009;89A:865–875.
11. He W, Ma Z, Teo WE, Dong YX, Robless PA, Lim TC, Ramakrishna S. Tubular nanofiber scaffolds for tissue engineered small-diameter vascular grafts. J Biomed Mater Res 2009;90A:205–216.
12. Prabhakaran MP, Venugopal JR, Ramakrishna S. Mesenchymal stem cell differentiation to neuronal cells on electrospun nanofibrous substrates for nerve tissue engineering. Biomaterials 2009; 30:4996–5003.
13. Vaquette C, Kahn C, Frochot C, Nouvel C, Six JL, De Isla N, Luo LH, Cooper-White J, Rahouadj R, Wang XO. Aligned poly(L-lactic-*co*-e-caprolactone) electrospun microfibers and knitted structure: A novel composite scaffold for ligament tissue engineering. J Biomed Mater Res 2010;94A:1270–1282.
14. He W, Ma ZW, Yong T, Teo WE, Ramakrishna S. Fabrication of collagen-coated biodegradable polymer nanofiber mesh and its potential for endothelial cells growth. Biomaterials 2005;26: 7606–7615.
15. Lim JI, Yu B, Lee YK. Fabrication of collagen hybridized elastic PLCL for tissue engineering. Biotechnol Lett 2008;30:2085–2090.
16. Ananta M, Aulin CE, Hilborn J, Aibibu D, Houis S, Brown RA, Mudera V. A poly(lactic acid-*co*-caprolactone)-collagen hybrid for tissue engineering applications. Tissue Eng Part A 2009;15: 1667–1675.
17. He W, Yong T, Teo WE, Ma ZW, Ramakrishna S. Fabrication and endothelialization of collagen-blended biodegradable polymer nanofibers: Potential vascular graft for blood vessel tissue engineering. Tissue Eng 2005;11:1574–1588.
18. Lee J, Tae G, Kim YH, Park IS, Kim SH. The effect of gelatin incorporation into electrospun poly(L-lactide-*co*-epsilon-caprolactone) fibers on mechanical properties and cytocompatibility. Biomaterials 2008;29:1872–1879.
19. Chen F, Li XQ, Mo XM, He CL, Wang HS, Ikada Y. Electrospun chitosan-P(LLA-CL) nanofibers for biomimetic extracellular matrix. J Biomater Sci Polym E 2008;19:677–691.
20. Zhang KH, Wang HS, Huang C, Su Y, Mo XM, Ikada Y. Fabrication of silk fibroin blended P(LLA-CL) nanofibrous scaffolds for tissue engineering. J Biomed Mater Res 2010;93A:984–993.
21. Mosesson MW. Fibrinogen and fibrin structure and functions. J Throm Haemost 2005;3:1894–1904.
22. Shaikh FM, Callanan A, Kavanagh EG, Burke PE, Grace PA, McGloughlin TM. Fibrin: A natural biodegradable scaffold in vascular tissue engineering. Cells Tissues Organs 2008;188:333–346.
23. McManus M, Boland E, Sell S, Bowen W, Koo H, Simpson D, Bowlin G. Electrospun nanofibre fibrinogen for urinary tract tissue reconstruction. Biomed Mater 2007;2:257–262.
24. McManus MC, Boland ED, Simpson DG, Barnes CP, Bowlin GL. Electrospun fibrinogen: Feasibility as a tissue engineering scaffold in a rat cell culture model. J Biomed Mater Res 2007;81A: 299–309.
25. Wnek GE, Carr ME, Simpson DG, Bowlin GL. Electrospinning of nanofiber fibrinogen structures. Nano Lett 2003;3:213–216.
26. Eyrich D, Brandl F, Appel B, Wiese H, Maier G, Wenzel M, Staudenmaier R, Goepferich A, Blunk T. Long-term stable fibrin gels for cartilage engineering. Biomaterials 2007;28:55–65.
27. Osathanon T, Linnes ML, Rajachar RM, Ratner BD, Somerman MJ, Giachelli CM. Microporous nanofibrous fibrin-based scaffolds for bone tissue engineering. Biomaterials 2008;29:4091–4099.
28. Kitajima T, Sakuragi M, Hasuda H, Ozu T, Ito Y. A chimeric epidermal growth factor with fibrin affinity promotes repair of injured keratinocyte sheets. Acta Biomater 2009;5:2623–2632.
29. Pankajakshan D, Philipose LP, Palakkal M, Krishnan K, Krishnan LK. Development of a fibrin composite-coated poly(epsilon-caprolactone) scaffold for potential vascular tissue engineering applications. J Biomed Mater Res B Appl Biomater 2008;87:570–579.
30. McManus MC, Boland ED, Koo HP, Barnes CP, Pawlowski KJ, Wnek GE, Simpson DG, Bowlin GL. Mechanical properties of electrospun fibrinogen structures. Acta Biomater 2006;2:19–28.
31. Sell SA, Francis MP, Garg K, McClure MJ, Simpson DG, Bowlin GL. Cross-linking methods of electrospun fibrinogen scaffolds for tissue engineering applications. Biomed Mater 2008;3: 45001–45012.
32. He CL, Zhang L, Wang HS, Zhang F, Mo XM. Physical-chemical properties and in vitro biocompatibility assessment of spider silk, collagen and polyurethane nanofiber scaffolds for vascular tissue engineering. Nano Biomed Eng 2009;1:119–129.
33. He CL, Xiao GY, Jin XB, Sun CH, Ma PX. Electrodeposition on nanofibrous polymer scaffolds: Rapid mineralization, tunable calcium phosphate composition and topography. Adv Funct Mater 2010;20:3568–3576.
34. He CL, Huang ZM, Han XJ. Fabrication of drug-loaded electrospun aligned fibrous threads for suture applications. J Biomed Mater Res 2009;89A:80–95.
35. Rejinold NS, Muthunarayanan M, Deepa N, Chennazhi KP, Nair SV, Jayakumar R. Development of novel fibrinogen nanoparticles by two-step co-acervation method. Int J Biol Macromol 2010;47: 37–43.
36. Inai R, Kotaki M, Ramakrishna S. Deformation behavior of electrospun poly(L-lactide-*co*-epsilon-caprolactone) nonwoven membranes under uniaxial tensile loading. J Polym Sci Polym Phys 2005;43:3205–3212.
37. Martins A, Pinho ED, Faria S, Pashkuleva I, Marques AP, Reis RL, Neves NM. Surface modification of electrospun polycaprolactone nanofiber meshes by plasma treatment to enhance biological performance. Small 2009;5:1195–1206.
38. Pektok E, Nottelet B, Tille J, Gurny R, Kalangos A, Moeller M, Walpoth B. Degradation and healing characteristics of small-diameter poly(e-caprolactone) vascular grafts in the rat systemic arterial circulation. Circulation 2008;118:2563–2570.
39. Sell S, Barnes C, Simpson D, Bowlin G. Scaffold permeability as a means to determine fiber diameter and pore size of electrospun fibrinogen. J Biomed Mater Res 2008;85A:115–126.